

# Residual stress measurement of Sic fiber /YSZ composite thermal barrier coating by micro-Raman spectroscopy

Rongbin Ma, Ziyi Tan and Genglei Kang

Key Laboratory of Micro-Nano Materials for Energy Storage and Conversion of Henan Province, Institute of Surface Micro and Nano Materials, Xuchang University, Xuchang, P. R. China  
Email: marongbinss@163.com

**Abstract.** Residual stress distribution in Sic fiber/YSZ composite thermal barrier coating (TBC) on a stainless substrate has been measured by micro-Raman spectroscopy. Stress-spectroscopic coefficient was calibrated on a independent TBC layer. The coefficient for all TBC system is  $\Sigma=33.92\text{cm-1Gpa-1}$ . The stress measurement along the TBC thickness shows compressive stress distribution is decrease progressively from substrate/top coat interface to TBC surface. And the fiber can effectively relaxing the residual stress of composite coating.

## 1. Introduction

Thermal barrier coating (TBC) has been widely used for turbine and aerial craft to protect components high temperature environment[1-3].The performance and lifetime of TBC are strongly affected by the condition of residual stress stored in TBC layer because these stresses lead to cracking of the coating layer, shape change and spallation during service. Thus, it is of a great importance to measure the residual stress of TBC. The stress has been measured by different experimental techniques.

The X-ray diffraction technique has been widely applied as a non-destructive method. The method is effective for measuring averaged stress in the TBC layer because the resolution of stress of is approximately 20MPa and spatial resolution is larger than 100 $\mu\text{m}$  and 20 $\mu\text{m}$  for in-plane and through-the-thickness directions, respectively[4]. The neutron diffraction is similar to the X-ray diffraction. The curvature method[4,5] can detect the curvature change of the TBC layer coated on a substrate. This technique is destructive and allows only macroscopic in-plane stress measurement; the spatial resolution for the through-the-thickness direction being 10-50% of the total specimen thickness[6,7]. And the substrate removal and strain measurement technique are useful engineering methods and are already being used for various kinds of TBC. The disadvantage of these techniques is the difficulty in measuring the local residual stress. The Raman spectroscopy is an effective method for measuring stresses in  $\text{ZrO}_2$  and has been applied to local stress measurement in TBC layer[8-11]. The spectroscopic technique usually uses a few micron-meter order laser beam as an excitation source.

The ultimate objective of TBC application is an improvement in efficiency by having an increase in the operating temperature. Increase the thickness of TBC can improvement the operating temperature, but the residual stress is proportional to the thickness of coating[12]. The top coat thickness of TBC is generally less than 2mm. But, the thickness of Sic fiber/YSZ composite TBC layer more than 4mm.



## 2. Experimental Procedures

### 2.1. Specimen Preparation and Coating Deposition

The 8wt% Y<sub>2</sub>O<sub>3</sub> stabilized ZrO<sub>2</sub>(YSZ), NiCoCrAlY and a composite powders (A mixture of amorphous SiO<sub>2</sub>, Al<sub>2</sub>O<sub>3</sub> and ZrO<sub>2</sub> powders with 7:3:90 weight ratio) were used to prepare the TBC samples. The NiCoCrAlY bond coat ( $\approx$ 150 $\mu$ m) layer had a chemical composition (wt%) of: 32.0-Ni, 39.5-Co, 21.0-Cr, 8.0-Al, and the remainder Y. The stainless substrates ( $\approx$ 2.5mm) were grit-blasted using Al<sub>2</sub>O<sub>3</sub> particles followed by ultrasonic cleaning in acetone for 20 min prior to air plasma spraying process. The spraying was conducted using a 40kW plasma torch (APS-3000, China National Aviation Corp, CHINA) according to parameters summarized in Table 1.

**Table 1.** The product conditions of plasma spraying

Spraying condition	Parameter
Are current [A]	450
Primary plasma gas flow [L/min]	Ar(0.55)
Secondary plasma gas flow [L/min]	N <sub>2</sub> (0.3)
Powder carrier gas	N <sub>2</sub>
Powder feed rate [g/min]	20
Spray distance [mm]	85



**Figure. 1** SEM observation showing the cross-section of the Sic fiber/ZrO<sub>2</sub> composite TBC layer

The as-deposited 4.2mm-thick Sic fiber/YSZ composite TBC system was cut into adequate size, then embedded in epoxy resin for polishing process. Thereafter, cross sectional surfaces of the TBC specimen were carefully polished up to 1 $\mu$ m diamond paste finish. The embedded TBC was dipped into dichloromethane to dissolve epoxy resin. And the specimen was dipped into 50wt% ferric solution at room temperature and the substrate alloy was slowly etched. The surplus of TBC layer was carefully cleaned with distilled water and dried by air blow, then the specimens were put into the holding furnace annealing treatment. The final size of the specimen was 5mm $\times$ 5mm $\times$ 4.2mm thick, it is defined as independent TBC. Fig. 1 show cross-section of the Sic fiber/YSZ composite TBC layer observed by scanning electron microscope (SEM); it contains many long fiber, and compared with the YSZ area the fiber area is loose. Direct calibration of the Raman peak around 640cm<sup>-1</sup> (tetragonal phase) was implemented on a independent coating and the Raman peak was then applied to a full TBC

system. The Raman peak shift was used for measurement entire TBC system the reason is discussed later.

### 2.2. Raman Spectroscopy

Raman spectroscopy was done using two kinds of specimens: a independent TBC layer and a TBC layer coated on a stainless substrate. A independent specimen was annealed to eliminate residual stress, which was placed on the Raman measuring equipment (IVVIA: special version RENISHAW Co., Britain) and the averaging the testing values of repeated measurements was used as Raman peak of standard.

Raman spectroscopic measurements were made at a fully controlled temperature ( $297\pm 1\text{k}$ ) in ambient air. A green laser (wavelength:  $\lambda=514.5\text{nm}$ ) was used as an excitation source of Raman spectroscopy and the beam was incident perpendicular to coating direction of the TBC layer. The Spacial Resolution: lateral  $1\mu\text{m}$  and depth  $1\mu\text{m}$ , and spectral repeatability of the spectrometer was less than  $0.2\text{ cm}^{-1}$  throughout the measured Raman shift range (from  $600$  to  $700\text{ cm}^{-1}$ ). This equipment was employed only for this wide range measurement. The origin of these peaks has been reported to be the tetragonal phase of  $\text{ZrO}_2$  and the peaks around  $640\text{cm}^{-1}$  were used for stress analysis of  $\text{ZrO}_2$  because of the high S/N ratio; this peak has been used for stress measurement of  $\text{Y}_2\text{O}_3$  stabilized  $\text{ZrO}_2$ <sup>[10,11]</sup>. In addition, high S/N ratio helps rapid measurement to avoid heating due to laser irradiation. The obtained Raman spectra were analyzed using OriginPro8.0 software which uses a Gaussian function via computer curve fitting. The spectroscopic conditions for the full TBC system are same as that for independent coating.

The micro-Raman spectroscopy is hard to quantitative analysis residual stress, so we are supplemented by X-ray diffraction. The residual stress measurements followed the general procedure outlined in Ref.[13].

### 3. Theoretical Analysis of the Residual Stress

Residual stresses in a plasma-sprayed TBC are generated through three events, namely phase transformation, rapid contraction of sprayed splats, and mismatch of thermal expansion coefficients of the substrate and coatings[13]. Stresses due to phase transformation, both from liquid to solid phase and solid state transformation in a typical top coat  $\text{ZrO}_2$  are negligible[13]. And  $\text{Y}_2\text{O}_3$  stabilized  $\text{ZrO}_2$  has been commonly used as the top coat of TBC system where the transformation of  $\text{ZrO}_2$  phase, from tetragonal to monoclinic phase and vice versa, is suppressed. The effect of the phase change is ignored. The second contributing component to the overall residual stress is quenching stress, which is due to rapid contraction of the sprayed splats as they are rapidly cooled from processing temperature to substrate temperature, the quenching stress  $\sigma_q$  can be estimated from [14]:

$$\sigma_q = \alpha_c (T_m - T_s) E_c \quad (1)$$

where  $\alpha_c$ ,  $E_c$ ,  $T_m$ ,  $T_s$  are coefficient of thermal expansion (CTE) of coating, elastic modulus of coating, meltingpoint of the sprayed material and substrate temperature, respectively. This type of residual stress can be eliminated by sufficient annealing treatment.

The third component of residual stresses is differential thermal contraction (DTC) stress that arises as the substrate and coating cool together from processing temperature. DTC stress is also known as thermal stress, and is induced by the mismatch in CTE of the substrate and sprayed materials. The thermal stress  $\sigma_t$  can be estimated by[15,16]:

$$\sigma_t \approx E_c \Delta\alpha \Delta T \frac{1+\nu}{1-\nu^2} \quad (2)$$

where  $E_c$ ,  $\Delta\alpha$ ,  $\Delta T$  and  $\nu$  are a the elastic modulus of coating, CTE mismatch between the substrate and coating, temperature difference upon cooling and the Poisson's ratio of coating, respectively. This residual stress for independent TBC specimen can be eliminated by sufficient annealing treatment, because independent TBC specimen is not include stainless substrate. Based on the above discussion,

Direct calibration of the Raman peak of the independent coating and the Raman peak was then applied to a full TBC system.

The overall magnitude of residual stress  $\sigma_r$  in TBC layer is given by:

$$\sigma_r = \sigma_q + \sigma_t \quad (3)$$

## 4. Results and Discussion

### 4.1. Raman Peak of Independent TBC

The Raman peak of independent TBC layer in the different annealing temperature and annealing time were listed in Table 2. These specimens are slowly cooled from annealing temperature and ambient temperature in the heat treatment furnace. It should be noted that the spectra are processed using GRAMS; this process does not affect peak location of the spectra. The data indicated that the magnitude of Raman peak in independent TBC specimen is a approximate constant when the annealing temperature is 897k and annealing time is 2h, in other words, the residual stress is  $\sigma_r \approx 0$  and the peak wavenumber from the independent TBC layer is  $\nu_0 = 635.509 \text{ cm}^{-1}$ . The peak wave was applied to full TBC system, although the calibration is a bit lower than the Raman peak of  $\text{Y}_2\text{O}_3$  stabilized  $\text{ZrO}_2$  ( $636.559 \text{ cm}^{-1}$ ). This difference come from the impacts of airflow and powder forming in the process of plasma spraying. This type of stress destined not the category of TBC residual stress.

**Table 2.** The Raman peak of independent TBC layer ( $\text{cm}^{-1}$ )

Annealing time, t(h)	Annealing temperature, T(k)					
	297k	497k	697k	897k	1097k	1297k
0h	636.357	-	-	-	-	-
1h	-	636.268	636.390	635.571	635.768	635.863
2h	-	636.254	636.192	635.509	635.509	635.509
3h	-	636.357	635.941	635.509	635.559	635.571
4h	-	636.357	635.558	635.519	635.509	635.592

This result clearly demonstrates that the Raman peak position with not residual stress, stress is measurable using Raman shift at a wavenumber around  $640 \text{ cm}^{-1}$ . The relationship between residual stress ( $\sigma_r$ ) and Raman peak frequency shift ( $\Delta\nu$ ) is written as:

$$\Delta\nu = \Sigma \sigma_r \quad (4)$$

Where stress-spectroscopic coefficient  $\Sigma$  is the constant,  $\sigma_r$  is the residual stress of TBC layer.

Fig. 2 is a example of Raman shift of a independent TBC layer without annealing treatment and under the 897k annealing with heat preservation 2h. The peak wave from the no annealing TBC layer is  $\nu = 638.357 \text{ cm}^{-1}$  and that annealing specimen is  $635.509 \text{ cm}^{-1}$ . This result clearly that indicates that the Raman peak position shift before and after annealing, in other words, the release of residual stress go with annealing. Based on the relationship between Raman peak shift and state of stress, the residual stress of TBC layer is compressive stress. Using the X-ray diffraction analysis equipment, we can know that the residual stress of independent TBC layer after annealing reduce by about 25Mpa. stress-spectroscopic coefficient  $\Sigma = 33.92 \text{ cm}^{-1} \text{ Gpa}^{-1}$  is calculated using Eq(4). It was reported that the stress-spectroscopic coefficient for PVD TBC and EB-PVD TBC were found to be  $4.55 \text{ cm}^{-1} \text{ Gpa}^{-1}$  [4] and  $5.43 \text{ cm}^{-1} \text{ Gpa}^{-1}$  [11], respectively. But, it should be noted that the coefficient has different meaning and condition from that reported in the literature because the independent TBC layer has different porosity and microstructure. Besides that, in previous studies on plasma-sprayed TBC, appreciably large coefficients have been observed. The coefficient for plasma-sprayed TBC was found to be  $25 \text{ cm}^{-1} \text{ Gpa}^{-1}$  [10], because the plasma-sprayed TBC has a higher porosity. The coefficient obtained from Sic fiber/YSZ composite TBC in the study is higher that from a typical plasma-sprayed TBC, it is probably due to loose fiber area as shown in Fig .1.

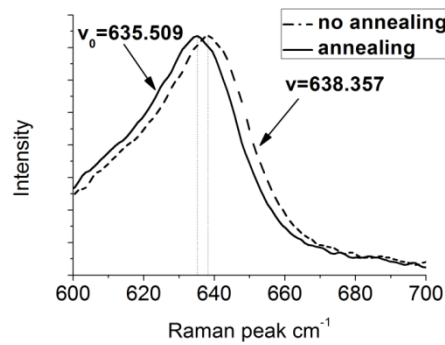


**Figure 2.A** example of Raman shift of a independent TBC layer before and after annealing

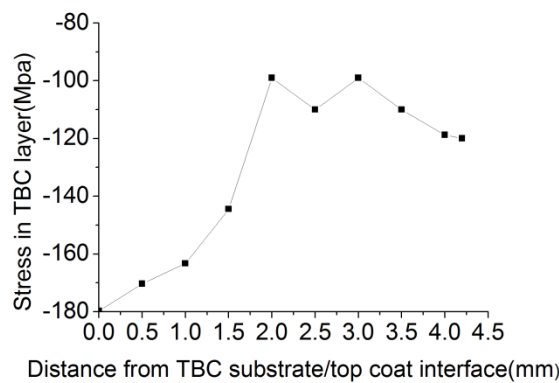


**Figure 3.** Residual stress distribution in through the thickness direction of the TBC layer

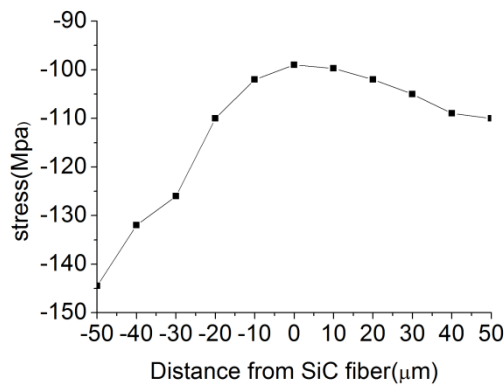


**Figure.4.** Residual stress distribution in fiber area (the direction from fiber toTBC top surface is defined as positive )

Fig.3 shows the residual stress distribution in the TBC layer along the through-the-thickness direction by using the stress-spectroscopic coefficient obtained previously. It is clear that the residual stress is compressive stress in all TBC system. Fig.4 shows the fiber takes effect to residual stress distribution. These results will be discussed below.

- The maximum residual stress was indentified at the substrate/Top-coat interface, the stress of TBC top surface is about -120MPa, it is close to that from X-ray diffraction data.
- The stress dependence on the distance from the TBC substrate/top -coat interface is same trend from that reported in Rsf. [17-19]. The magnitude of stress from top coat surface to substrate is decrease progressively. As shown in Fig.3, there is an extreme valuee when the distance is about 2mm, This is due to the fiber reinforced coatings of ductile behavior, creep

and plasticity, these performance are dominant in relaxing stresses. From the Fig.4 shows the areas of near fiber has lower residual stress.

- The stress level of all TBC system fall with in arrange of -180~-120MPa, which is about six times bigger than the stress from Ref. [20]. Because the residual stress of TBC layer is in proportion to the coating thickness. Relative to the thickness (4.2mm) of top coat in this study, the top coat thickness just only hundreds of micrometers.

## 5. Conclusions

Residual stress in Sic fiber/YSZ composite TBC on a stainless steel substrate has been measured by micro-spectroscopic method. The stress-spectroscopic coefficient  $\Sigma=33.92\text{cm-1Gpa-1}$  was then used to residual stresses in the TBC layer of a full TBC system. The residual stress of TBC layer was found to be within -180~-120MPa. Near the areas of fiber the stress has a minimum value due to the fiber effect the coatings of ductile behavior, creep and plasticity. This study showed that the fiber can effectively relaxing the residual stress of composite coating, and the effectiveness of micro-Raman spectroscopy for the measurement of residual stress in plasma-sprayed Sic fiber/YSZ composite TBC layer.

## Acknowledgments

ReferThe authors gratefully acknowledge to Prof Xudong Cheng for many constructive suggestions.

## References

- [1] Miller and Robert A1994 J.Am. Ceram.Soc. **67** 517
- [2] Miller and RobertA1997 J.Am. Ceram.Soc. **6** 35
- [3] P. Scardi, M. Leoni, L and Bertamin 1995 Surf. Coat. Technol.**76-771** 06
- [4] V. Teixeira and M. Andritschky 1999 Journal of Materials Processing Technology **92-93** 209
- [5] M.K. Hobbs, H. Reiter 1998 Surf. Coat. Technol. **34** 33
- [6] S. Krämer, S. Faulhaber, M. Chambers, D.R. Clarke, C.G. Levi, J.W. Hutchinson and A.G. Evans 2008 Mater. Sci. Eng. A. **490** 26
- [7] A. Scrivani and G.. Rizzi 2007 J. Them. Spray. Technol. **16** 816
- [8] Jiguang Cai and Y. S. Raptis 1993 Applied Physics Letters. **62** 2781
- [9] P. Bouvier and G. Lucazeau 2000 Journal of Physics and Chemistry of Solids. **61** 569
- [10] M. Tanaka and M. Hasegawa 2006 Mater. Sci. Eng. A . **419** 262
- [11] M. Tanalca and R. Kitazawa 2009 Surf. Coat. Technol. **204** 657
- [12] M. Levit and L. Grimberg 1996 Materials Science and Engineering A. **206** 30
- [13] Sujanto Widjaja and M. Limarga 2003 Thln Snlidd Fdlms.**434** 216
- [14] Rongbin Ma and Xudong Cheng 2015 Applied Surface Science. **357** 407
- [15] J.D. Lee and H.Y. Ra 1992 Advanced Materials & Processes. **56** 27
- [16] Shaw, L.L 1997 Composites B. **29** 199
- [17] MA Rong-Bin and CHENG Xu-Dong 2016 Journal of Inorganic Materials. **31** 190
- [18] Biakas. M 2008 Surf. Coat. Technol. **202** 6002
- [19] Yongle Sun and Jianguo Li 2013 Surface & Coatings Technology. **216** 237
- [20] Khan A.N and LuJ, Liao H 2003 Surf. Coat. Technol. **168** 291